

CONTROL-RELEVANT SOFC MODELING AND MODEL EVALUATION

Rambabu Kandepu*, Lars Imsland*, Bjarne A. Foss*
Department of Engineering Cybernetics
Christoph Stiller†, Bjørn Thorud† and Olav Bolland†
Department of Process Engineering
Norwegian University of Science and Technology
7491 Trondheim, Norway

ABSTRACT

In this paper, a dynamic, lumped model of a Solid Oxide Fuel Cell (SOFC) is described, as a step towards developing control relevant models for a SOFC integrated in a gas turbine process. Several such lumped models can be aggregated to approximate the distributed nature of important variables of the SOFC. The model is evaluated against a distributed dynamic tubular SOFC model. The simulation results confirm that the simple model is able to capture the important dynamics of the SOFC. It is concluded that the simple model can be used for control and operability studies of the hybrid system.

Keywords: SOFC, control relevant, fuel cells, modeling

INTRODUCTION

Solid Oxide Fuel Cells (SOFC) integrated in Gas Turbine (GT) cycles (often denoted hybrid systems) is a promising concept for production of efficient and low-polluting electrical power. The SOFC can produce electric power at an electrical efficiency of about 55%, and when it is combined with a GT, studies show that the net electrical efficiency can be increased up to 70% [8]. The hybrid system uses natural gas as fuel and the percentage of pollutant flue gases is low compared to conventional power production from fossil fuels.

Due to the tight integration between the SOFC and the GT in a hybrid system, dynamic operability (and hence control) of the process is a challenge. It is important not only to design a good control system, but also to choose a process design that together with the appropriate control structure allows satisfying disturbance rejection and part load operation. Such a design procedure is usually called a integrated process design, see eg. van Schijndel [15]. To be able to design control structures and analyze dynamic behavior, it is very beneficial to have low complexity models of the components of the hybrid system. Such models are also valuable for online optimization. The aim of this article is to develop a

low complexity mechanistic SOFC dynamic model which includes the relevant dynamics for operation in a hybrid system. There are several dynamic, distributed models reported in the literature. For example, Achenbach [1] developed a three dimensional, dynamic, distributed model for a planar SOFC stack. Chan et al. [4, 3], Thorud et al. [14], Stiller et al. [12] and Magistri et al. [10] all developed distributed, dynamic tubular SOFC models for designs similar to that of Siemens Westinghouse, for use in hybrid systems. In this paper, a simple, lumped, dynamic model of the SOFC based on mass and energy balances, with methane as fuel, is developed. The modeling approach proposed by Padulles et al. [11] for use in power systems simulation has some similarities with the approach described in this paper, however, therein hydrogen is used as fuel and only mass balances are considered.

The paper is outlined as follows: First a simple control relevant SOFC model is described with no regard to the geometric layout (tubular or planar). Extension of the simple lumped model towards capturing the distributed nature of the process by aggregating single volumes is explained next. Both SOFC models are evaluated against a distributed tubular SOFC model [14] with a considerably higher complexity. The two models are simulated for different realistic scenarios and the corresponding simulation results are presented. Applicability and shortcom-

*{Rambabu.Kandepu,Lars.Imsland,Bjarne.A.Foss}@itk.ntnu.no

†{Christoph.Stiller,Bjorn.Thorud,Olav.Bolland}@ntnu.no

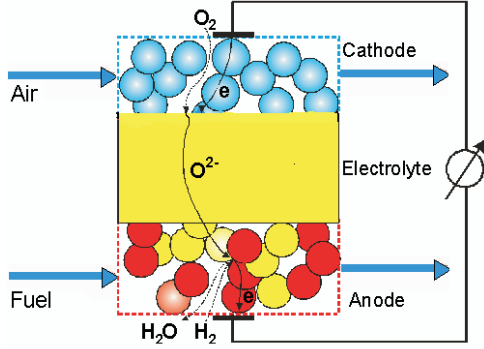


Figure 1: SOFC operation

ings of the low complexity model are discussed. A nomenclature can be found at the end of the paper.

PROCESS DESCRIPTION

The Solid Oxide Fuel Cell (SOFC) is a device which converts chemical energy of a fuel directly into electrical energy [7]. The basic components of the SOFC are anode, cathode and electrolyte (conceptually illustrated in Figure 1). The electrolyte material is zirconia stabilized with the addition of a small percentage of yttria (Y_2O_3). The anode material is a zirconia cermet. The most common cathode material is strontium-doped lanthanum manganite. Fuel is supplied to the anode and air is supplied to the cathode. At the cathode-electrolyte interface, oxygen molecules accept electrons coming from the external circuit to form oxide ions, see Table 1 for reactions. The electrolyte layer allows only oxide ions to pass through and at the anode-electrolyte interface, hydrogen molecules present in the fuel react with oxide ions to form steam and electrons get released. These electrons pass through the external circuit and reach the cathode-electrolyte layer, and thus the circuit is closed. To increase the amount of power generated, a number of cells can be connected in series/parallel. This is known as stacking of cells. Also, there are mainly two types of SOFCs depending on the geometry; tubular and planar. The operating pressure can be from one bar to 15 bars. It is found that SOFCs show enhanced performance with increasing cell pressure [7]. The operating temperature of the SOFC is around 800-1000°C. The high temperature and pressure operating conditions of the SOFC make it advantageous to combine the SOFC with a gas turbine (GT) to get a hybrid system with an high efficiency [8]. Due to the high operating temperature, an advantage is that several types of

Table 1: Reactions at anode and cathode

| At anode | |
|--|------------------------------|
| Reaction | Reaction rate (r_j^{an}) |
| $H_2 + O^{2-} \rightarrow H_2O + 2e^-$ | r_1^{an} |
| $CH_4 + H_2O \Leftrightarrow CO + 3H_2$ | r_2^{an} |
| $CO + H_2O \Leftrightarrow CO_2 + H_2$ | r_3^{an} |
| $CH_4 + 2H_2O \Leftrightarrow CO_2 + 4H_2$ | r_4^{an} |
| At cathode | |
| Reaction | Reaction rate (r_j^{ca}) |
| $\frac{1}{2}O_2 + 2e^- \rightarrow O^{2-}$ | r_1^{ca} |

fuels can be used. In this paper methane is used as fuel. Because of the electrochemical reactions, there is a production of steam, and partial recirculation of this steam is used to reform methane into hydrogen. Typically, one third of the fuel is reformed (for example, in a pre-reformer) before it enters the SOFC and the remaining part is reformed within the SOFC. Table 1 gives the list of reactions that take place at anode and cathode and the corresponding reaction rates notation.

MODELING

The dynamic model of a single SOFC is developed using two mass balances; one for anode volume and the other for cathode volume, and one overall energy balance. In all of the streams from/to the SOFC, the following components can be present; Nitrogen (N_2), Oxygen (O_2), Hydrogen (H_2), Methane (CH_4), Steam (H_2O), Carbonmonoxide (CO), and Carbondioxide (CO_2). A number is assigned to each of these components to simplify the notation:

| i | 1 | 2 | 3 | 4 | 5 | 6 | 7 |
|-------|-------|-------|-------|--------|--------|----|--------|
| comp. | N_2 | O_2 | H_2 | CH_4 | H_2O | CO | CO_2 |

Model assumptions

The following main assumptions are made in developing the model.

1. All the physical variables are assumed to be uniform over the SOFC, resulting in a lumped model.
2. There is sufficient turbulence and diffusion within the anode and the cathode for perfect mixing to occur (CSTR).
3. The gas temperatures within the SOFC are assumed to be the same as the solid; i.e. the thermal inertia of the gases is neglected.

4. For the energy balance, pressure changes within the SOFC are neglected.
5. All gases are assumed to be ideal.

Mass balances

Two mass balances; one for the anode volume and one for the cathode volume are used:

$$\frac{dN_i^{an}}{dt} = \dot{N}_i^{in,an} - \dot{N}_i^{out,an} + \sum_{j=1}^{n_{rx}^{an}} a_{ij}^{an} r_j^{an}, \quad (1)$$

$$i = 1, \dots, 7, \quad n_{rx}^{an} = 4$$

$$\frac{dN_i^{ca}}{dt} = \dot{N}_i^{in,ca} - \dot{N}_i^{out,ca} + \sum_{j=1}^{n_{rx}^{ca}} a_{ij}^{ca} r_j^{ca}, \quad (2)$$

$$i = 1, \dots, 7, \quad n_{rx}^{ca} = 1$$

The reaction rates corresponding to the electrochemical reactions (r_1^{ca} , r_1^{an}) are directly related by the current,

$$r_1^{an} = I/(2F) = r_1^{ca} \quad (3)$$

and the reaction rates corresponding to the reforming reactions are calculated as proposed by Xu [16]

$$r_2^{an} = \frac{k_2}{P_{H_2}^{an^{2.5}}} \left(P_{CH_4}^{an} P_{H_2O}^{an} - \frac{P_{H_2}^{an^3} P_{CO}^{an}}{K_2} \right) / (DEN)^2$$

$$r_3^{an} = \frac{k_3}{P_{H_2}^{an}} \left(P_{CO}^{an} P_{H_2O}^{an} - \frac{P_{H_2}^{an} P_{CO_2}^{an}}{K_3} \right) / (DEN)^2 \quad (4)$$

$$r_4^{an} = \frac{k_4}{P_{H_2}^{an^{3.5}}} \left(P_{CH_4}^{an} P_{H_2O}^{an^2} - \frac{P_{H_2}^{an^4} P_{CO_2}^{an}}{K_4} \right) / (DEN)^2$$

In (4), DEN is given by

$$DEN = 1 + K_{CO}^{ads} P_{CO}^{an} + K_{H_2}^{ads} P_{H_2}^{an} + K_{CH_4}^{ads} P_{CH_4}^{an} + K_{H_2O}^{ads} P_{H_2O}^{an} / P_{H_2}^{an} \quad (5)$$

and k_2, k_3 and k_4 , the rate coefficients for the reforming reactions, are calculated by

$$k_j = A_{kj} \exp\left(\frac{-E_j}{RT}\right), \quad j = 2, 3, 4 \quad (6)$$

The equilibrium constants for the reforming reactions K_2, K_3 and K_4 are given by

$$\begin{aligned} K_2 &= \exp(-26830/T + 30.114) \quad [bar^2] \\ K_3 &= \exp(4400/T - 4.036) \quad [-] \\ K_4 &= \exp(-22430/T + 26.078) \quad [bar^2] \end{aligned} \quad (7)$$

In (5), $K_{CO}^{ads}, K_{H_2}^{ads}, K_{CH_4}^{ads}$ and $K_{H_2O}^{ads}$ are the adsorption constants, which are calculated by

$$K_i^{ads} = A_{K_{ads_i}} \exp\left(\frac{-\Delta\bar{h}_i^{ads}}{RT}\right), \quad i = H_2, CH_4, H_2O, CO \quad (8)$$

It is assumed that the exhaust flows at the anode and cathode outlets can be described by the choked exhaust flow equation. This means that the mass flow rate of the exhaust flow at the anode (cathode) depends on the pressure difference between the pressure inside the anode (cathode) and the pressure at the outlet [11]:

$$\dot{m}_{out,an} = \sqrt{k_{an}(p_{an} - p_{out,an})} \quad (9)$$

$$\dot{m}_{out,ca} = \sqrt{k_{ca}(p_{ca} - p_{out,ca})}$$

The partial pressures, volume, and temperature are assumed to be related by the ideal gas equation, for instance at the anode,

$$p_i^{an} V_{an} = N_i^{an} RT \quad (10)$$

Energy balance

The energy balance accounts for the whole SOFC volume, and is given by [13, 9]:

$$\begin{aligned} C^s \frac{dT}{dt} &= \sum_{i=1}^N \dot{N}_i^{in,an} (\Delta\bar{h}_i^{in,an} - \Delta\bar{h}_i) \\ &+ \sum_{i=1}^N (\dot{N}_i^{in,ca} (\Delta\bar{h}_i^{in,ca} - \Delta\bar{h}_i) \\ &- \sum_{j=1}^M \Delta\bar{h}_j^{rx} r_j^{an} - P_{DC} - P_{rad} - P_{cond} \end{aligned} \quad (11)$$

In this equation, the temperature changes of gases are neglected as they are fast compared to the temperature changes of the solid and by assuming that these fast changes of gas temperatures do not influence the dynamics of the overall process. Hence the energy balance gives a dynamic equation for the temperature changes of the SOFC solid.

In (11), P_{DC} represents the amount of DC power produced by the SOFC, P_{cond} represents the conduction heat loss from SOFC to the surroundings and P_{rad} represents the amount of radiation heat given from the SOFC. As the SOFC operating temperature is higher than that of the surroundings, there is always some loss due to radiation. It can be calculated by [6]

$$P_{rad} = A \delta \epsilon \sigma (T^4 - T_{sur}^4) \quad (12)$$

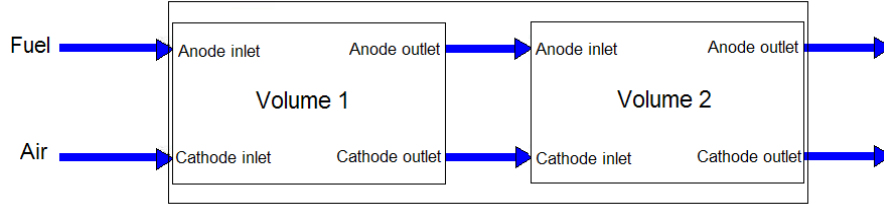


Figure 2: Aggregation mechanically

In (12), A is the surface area, δ is shaping factor, T_{sur} represents the surroundings temperature, ε is the emissivity of the SOFC surface and σ is the *Stefan-Boltzmann constant* ($\sigma = 5.67 \times 10^{-8} \text{W}/(\text{m}^2 \cdot \text{K}^4)$). The amount of DC power from the SOFC is given by

$$P_{DC} = VI \quad (13)$$

Voltage

The operating cell voltage is given by

$$V = E^{OCV} - V_{loss} \quad (14)$$

where the open circuit voltage of the cell is given by the *Nernst equation* [7],

$$E^{OCV} = E^o + \frac{RT}{2F} \ln \left(\frac{p_{H_2}^{an} p_{O_2}^{an0.5}}{p_{H_2O}^{an}} \right) \quad (15)$$

where E^o is the EMF at standard pressure. V_{loss} is the voltage loss, as explained below.

Voltage loss

When the cell is operated, there are voltage losses coming from different sources; activation losses, concentration losses and ohmic losses [7]. Activation losses are caused by the limited reaction rate on the surface of the electrodes. Ohmic losses are due to the electrical resistance of the electrode material and the various interconnections, as well as the resistance of the electrolyte. The ohmic losses are responsible for the largest part of the voltage losses. The concentration losses result from the change in concentration of the reactants at the surface of the electrodes as the fuel is used. Stiller et al. [12], Thorud et al. [14], Campanari et al. [2], and Magistri et al. [10] used rather complex empirical functions to calculate the ohmic and activation losses. In this simple model the total voltage loss is approximated by a first order function of cell temperature

and current. This function is obtained by curve fitting the simulated data obtained from a distributed model [14], where an active area of 834cm^2 is used to calculate the different voltage losses. Thus total voltage loss is calculated by

$$V_{loss} = f(I, T) \quad (16)$$

MODEL AGGREGATION

In a real SOFC, temperature and pressure vary over the SOFC volume. The distributed nature cannot be represented by using the "one volume" model. By connecting many volumes in a sequential manner it is possible to approximate the distributed nature of the variables. The whole structure with all the volumes represent a single cell. So, if many volumes are connected, each volume can be represented by a scaled-down model. In principle, it is possible to connect any number of volumes, but for simplification, an example is considered where a single SOFC model is obtained by connecting two scaled-down models as shown in Figure 2. The two volumes are selected such that the first volume is represented by a scaled-down model by scaling down the "one volume" model volume and heat capacity constants by $1/3$. The second volume is represented by a scaled-down model obtained by scaling down the "one volume" model constants by $2/3$. Electrically, the two scaled-down models are connected in parallel (Figure 3). Ideally, the voltage across each of the volumes should be the same and the total current is divided between the two volumes. Then probably, most of the current will be produced from the second volume, as mainly reforming reactions take place in the first volume. In the present work it is assumed that the first volume supplies $1/3$ rd of the total current and the second volume supplies the remaining current. With this assumption, there is a small voltage difference between the two volumes. Developing a strategy for dividing the currents among the volumes when a SOFC is represented by many volumes is a part of further work. The basic point is

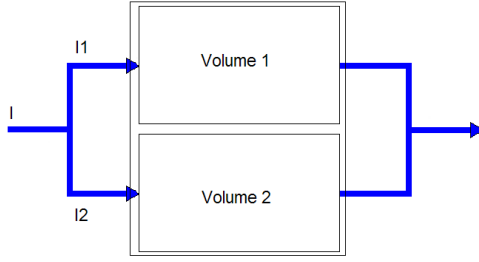


Figure 3: Electrical aggregation

to show that it is possible to approximate the distributed nature of the variables by aggregating the scaled-down models.

MODEL EVALUATION

As no experimental data is available to the authors for evaluating the simple model, the model is evaluated with an available detailed model. The detailed model [14] is a quasi two-dimensional dynamic model of a SOFC tube, similar to that of Siemens Westinghouse. It is a discretized model where gas flows are treated as 1D plug flows. The solid structures are modeled by a 2D discretization scheme in the axial and radial direction, neglecting effects in the circumferential direction. Both the simple and the detailed models are developed using gPROMS [5]. For solving the detailed model gPROMS uses about 1300 differential equations, whereas for the simple model it uses 15 differential equations.

Figure 4 shows the comparison set up used for the simulation. Here the main aim is to evaluate the simple model against the detailed model [14]. The simulations are performed in such a way that the same input conditions are applied to the two SOFC models. Fuel is supplied to the pre-reformer which reforms about 30% of methane. The pre-reformer outlet gas is supplied to the anode inlet and air is supplied to the cathode inlet. Some part of the anode flue gas is recycled back to the pre-reformer to supply steam required by the reforming reactions. The other part of the anode flue gas and the cathode flue gas are supplied to a combustor where the remaining fuel is burnt and the resultant gas mixture will be the exhaust gas. The SOFC and pre-reformer are thermally connected by radiation. The details of the models of the other components used in the process shown in Figure 4 are not discussed here. The values of important parameters of the simple model are given in Table 2. The values of important variables at steady state are given in Table 3. Table 4 shows

Table 2: Model parameters

| | |
|----------------|---|
| Anode volume | $1.032 \times 10^{-5} \text{m}^3$ |
| Cathode volume | $4.3 \times 10^{-5} \text{m}^3$ |
| C^s | 800J/K |
| k_{an} | $1.9 \times 10^{-3} \text{kg}^2 \text{s}^{-2} \text{Pa}^{-1}$ |
| k_{ca} | $4.2 \times 10^{-3} \text{kg}^2 \text{s}^{-2} \text{Pa}^{-1}$ |

Table 3: Steady state values

| | |
|---------------------------|-----------------------------------|
| methane flow rate | $4.50 \times 10^{-4} \text{kg/s}$ |
| methane inlet temperature | 950K |
| Air flow rate | $1.44 \times 10^{-2} \text{kg/s}$ |
| Air inlet temperature | 950K |
| Current | 250A |
| Anode pressure | 3bar |
| Cathode pressure | 3bar |
| Cell voltage | 0.56V |
| Cell power | 141W |
| Cell temperature | 1113K |
| air utilization | 0.21 |
| fuel utilization | 0.7 |

the simulation scenarios used for comparing the dynamic behavior of the two models.

SIMULATION RESULTS

Simulations are made for two comparison schemes; first, the simple SOFC model with one volume is compared to the distributed tubular SOFC model [14], and second, the simple SOFC with two volumes is compared to the distributed tubular SOFC model. SOFC mean solid temperature, cell voltage and cell power of the simple model and the detailed model are compared in each comparison scheme. Figures 5-7 show simulation results of the first comparison scheme and Figures 8-9 show simulation results of the second comparison scheme.

Table 4: Simulation details

| Time(min) | Disturbance |
|-----------|-------------------------------------|
| 90 | fuel flow is decreased by 20% |
| 180 | fuel flow is increased back to 100% |
| 270 | air flow is decreased by 20% |
| 360 | air flow is increased back to 100% |
| 450 | current is decreased by 20% |
| 540 | current is increased back to 100% |

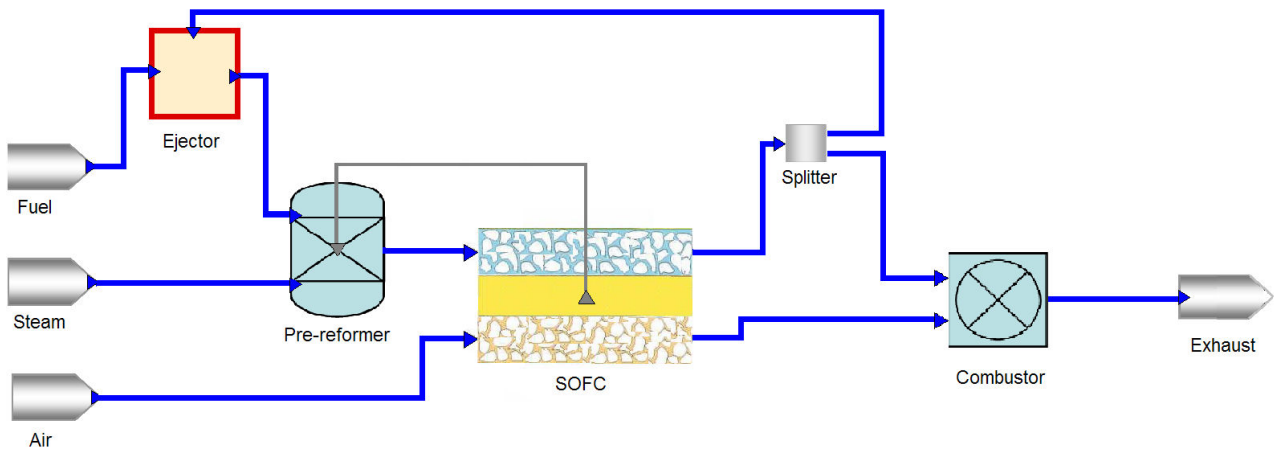


Figure 4: SOFC system

DISCUSSION

One volume SOFC model

Figure 5 shows the mean temperatures of the simple and the detailed SOFC models. At nominal steady state there is a temperature difference of about 120K between the two mean SOFC temperatures. This can be explained as follows. For both SOFC models, since inlet massflows and current are the same, the energy balance should ensure that the energy in the outlet massflow (and hence outlet temperature) is approximately¹ the same for both models. In a SOFC, the maximum temperature region is at the outlets of the anode and the cathode. Since the simple model is a bulk model, the exit temperature is equal to the mean temperature. For the detailed model, SOFC temperature is a distributed variable and the mean temperature is certainly less than the exit temperature. It is verified that the maximum temperature of the detailed model at the nominal steady state is approximately equal to the mean temperature of the simple SOFC model. From Figure 5, it is clear that both the models exhibit similar dynamics for the disturbances applied during the simulation. Figure 6 shows the voltages of the two models during the simulation. Here also both models show the same dynamic changes in the voltages for all the disturbances applied. Here the simple model has higher voltage than the detailed model which is also mainly because of the higher mean solid temperature of the simple SOFC model. Referring to (16), when temperature increases the voltage loss decreases. Hence the simple SOFC voltage given

¹A slight difference in voltage and hence produced DC power gives a small temperature difference.

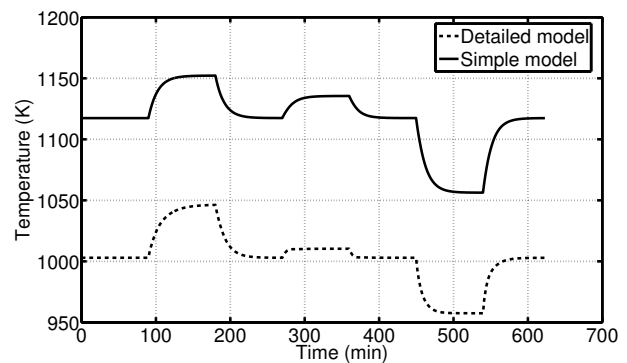


Figure 5: Comparison of mean solid temperatures of the simple model with one volume and the detailed model for different disturbances

by (14) is higher than that of the detailed SOFC model at the nominal steady state. Figure 7 shows a comparison of power production of the two models during the simulation. Since the voltage of the simple SOFC model is higher than that of the detailed model and the current is the same in both models, the power produced by the simple SOFC model is higher.

Two volume SOFC model

Figure 8 shows the comparison of the mean temperatures of the two SOFC models. Now, the simple SOFC is represented by aggregation of two volumes. The simple SOFC solid mean temperature is given by the average of the temperatures of the two volumes. The difference between the two mean temperatures at the nominal steady state is reduced to 51K as supposed to 120K. The dynamics of the two

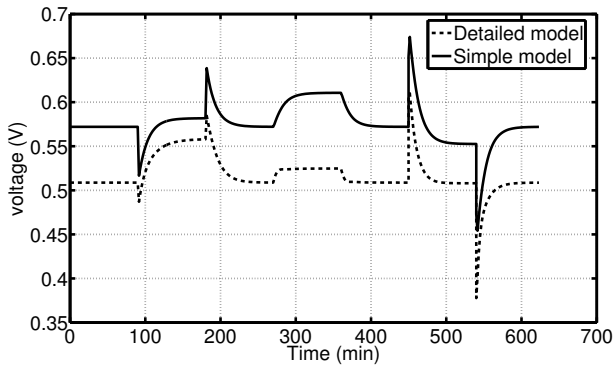


Figure 6: Comparison of voltages of the simple model with one volume and the detailed model for different disturbances

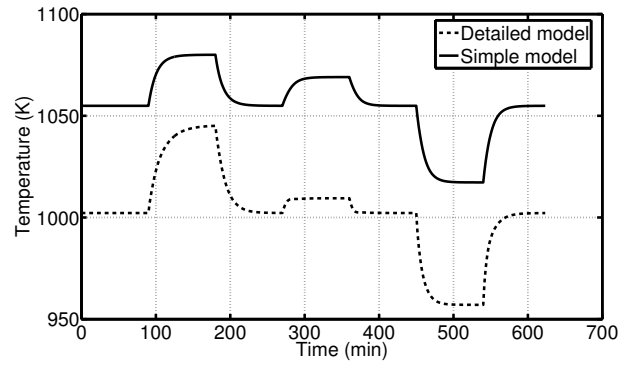


Figure 8: Comparison of mean solid temperatures of the simple model with two volumes and the detailed model for different disturbances

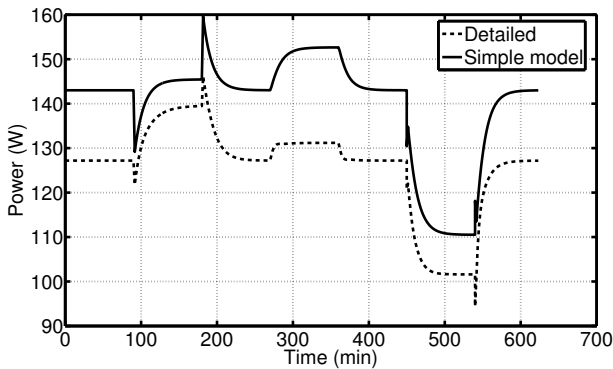


Figure 7: Comparison of power production of the simple model with one volume and the detailed model for different disturbances

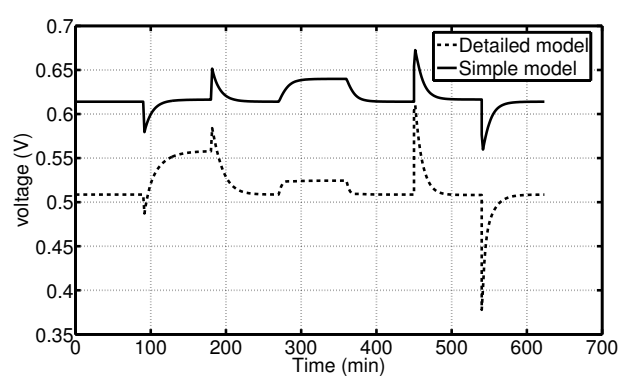


Figure 9: Comparison of voltages of the simple model with two volumes and the detailed model for different disturbances

volume model is similar to that the dynamics of the one volume model for all the disturbances. Figure 9 shows the comparison of the voltages of the two models, for the two volume model the average voltage is plotted. There is a small voltage difference of 0.1V between the two volumes and this is caused by the somewhat crude approximate distribution of currents between the two volumes. Developing a strategy for a more accurate distribution of currents between two or more volumes is a topic for future work.

CONCLUSION AND FURTHER WORK

From the simulation results, it is quite clear that even though there is some steady state offset, important variables of the simple and the detailed models show similar dynamic behavior during the simulations. It can therefore be concluded that the simple model is able to capture the overall dynamics of the SOFC.

This model will hence be used for further studies on control and operability of the hybrid system, i.e. an SOFC integrated in a GT cycle.

If the one volume model is too crude, it is possible to aggregate a number of volumes. The results herein however indicate that a one volume model may suffice in many cases.

Further work includes developing the simple models of the other components in the SOFC-GT hybrid system, looking at how different design decisions affect controllability and developing an optimizing control structure for safe and part load operation.

Acknowledgments

Financial support from The Gas Technology Center, NTNU-SINTEF is acknowledged.

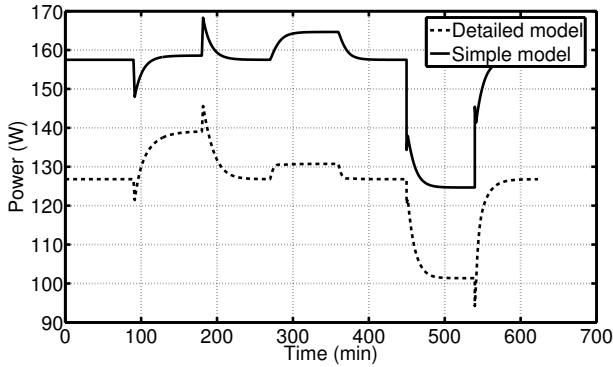


Figure 10: Comparison of powers of the simple model with two volumes and the detailed model for different disturbances

NOMENCLATURE

| | |
|------------------------------------|--|
| a_{ij} | stoichiometric matrix |
| A | SOFC surface area |
| $A_{k_i}, A_{K^{ads}}$ | pre-exp. factors for k_i |
| C^s | solid heat capacity |
| DEN | denominator |
| E | activation energy |
| E^o | EMF at standard temperature and pressure |
| E^{OCV} | open circuit voltage |
| F | Faraday's constant |
| I | current |
| k_2, k_3, k_4 | rate coefficients for reforming reactions |
| k_{an}, k_{ca} | choked flow constants |
| K_j | equilibrium constant for reaction j |
| K_i^{ads} | adsorption constant for component i |
| \dot{m} | mass flow rate |
| n_{rx} | number of reactions |
| N | number of moles |
| p | pressure |
| P | power |
| r_j | reaction rate of reaction j |
| R | universal gas constant |
| T | temperature |
| V_{an}, V_{ca} | volumes |
| V | voltage |
| $\Delta \bar{h}$ | molar specific enthalpy |
| $\Delta \bar{h}^{rx}$ | molar specific enthalpy change of reaction |
| $\Delta \bar{h}^{ads}$ | enthalpy change of adsorption |
| δ | shaping factor |
| Subscripts and superscripts | |
| i | chemical component |
| j | reaction |
| an | anode |
| ca | cathode |
| in | inlet |
| out | outlet |
| rad | radiation |
| $cond$ | conduction |

REFERENCES

- [1] E. Achenbach. Three-dimensional and time-dependent simulation of a planar solid oxide fuel cell stack. *Journal of Power Sources*, 1994.
- [2] S. Campanari. Thermodynamic model and parametric analysis of a tubular sofc module. *Journal of Power Sources*, 2004.
- [3] S.H. Chan, H.K. Ho, and Y. Tian. Modelling of a simple hybrid solid oxide fuel cell and gas turbine power plant. *Journal of Power Sources*, 2002.
- [4] S.H. Chan, H.K. Ho, and Y. Tian. Multi-level modeling of sofc-gas turbine hybrid system. *International Journal of Hydrogen Energy*, 2003.
- [5] gPROMS (2004). gPROMS introductory user guide. *Process Systems Enterprise Ltd.*, 2004.
- [6] F. P. Incropera and D. P. De Witt. *Fundamentals of Heat and Mass Transfer*. Wiley, USA, 2002.
- [7] J. Larminie and A. Dicks. *Fuel Cell Systems Explained*. Wiley, England, 2003.
- [8] J. Pålsson, A. Selimovic, and L. Sjunnesson. Combined solid oxide fuel cell and gas turbine systems for efficient power and heat generation. *Journal of Power Sources*, 2000.
- [9] M. D. Lukas, K. Y. Lee, and H. Ghezal-Ayagh. An explicit dynamic model for direct reforming carbonate fuel cell stack. *IEEE Transactions on Energy Conversion*, 16(3), September 2001.
- [10] L. Magistri, F. Trasino, and P. Costamagna. Transient analysis of a solid oxide fuel cell hybrids part a: fuel cell models. *Journal of Power Sources*, 2004.
- [11] J. Padulles, G.W. Ault, and J. R. McDonald. An integrated sofc dynamic model power systems simulation. *Journal of Power sources*, pages 495–500, 2000.
- [12] C. Stiller, B. Thorud, S. Seljebø, Ø. Mathisen, H. Karoliussen, and O. Bolland. Finite-volume modeling and hybrid-cycle performance of planar and tubular solid oxide fuel cells. *Journal of Power Sources*, 2004.
- [13] P. Thomas. *Simulation of Industrial Processes For Control Engineers*. Butterworth-Heinemann, Woburn, MA, USA, 1999.
- [14] B. Thorud, C. Stiller, T. Weydahl, O. Bolland, and H. Karoliussen. Part-load and load change simulation of tubular sofc systems. *Fuel Cell Forum, Lucerne, 28 June-2 July 2004*, 2004.
- [15] J. van Schijndel and E. N. Pistikopoulos. Towards the integration of process design, process control, and process operability: Current status and future trends. *In the proceedings of FOCPD '99, Breckenridge, Colorado, USA*, 1999.
- [16] J. Xu and G. F. Froment. Methane steam reforming, methanation and water-gas shift: I. intrinsic kinetics. *AIChE Journal*, 1989.